Magnetic behavior of superparamagnetic Fe nanocrystals confined inside submicron-sized spherical silica particles

P. Tartaj,* T. González-Carreño, O. Bomatí-Miguel, and C. J. Serna
Instituto de Ciencia de Materiales de Madrid, CSIC, Cantoblanco, 28049 Madrid, Spain

P. Bonville
CEA, CE Saclay, Service of Physique de l'Etat Condensé, 91191 Gif-sur-Yvette, France
(Received 20 May 2003; revised manuscript received 22 October 2003; published 8 March 2004)

We have studied the magnetic behavior of superparamagnetic Fe nanocrystals (4–7 nm in diameter) dispersed in submicron-sized spherical silica particles (~150 nm in diameter). Spherical composites that could be useful for biomedical applications were prepared by an aerosol-assisted method. Mössbauer studies have allowed us to determine that the magnetic response of the composites must be the result of a competition between intraparticle anisotropy and interparticle dipolar interactions. Evidence of an interacting superparamagnetic (ISP) regime that is characterized by a H/M_s scaling law of the reduced magnetization isotherms instead the H/T scaling law of the ideal superparamagnetic regime has been found in the composites. The ISP regime, as recently reported in similar nanostructured systems, appears as an intermediate regime, separating the high-temperature, conventional superparamagnetic regime from the low-temperature, blocked-particle regime. We have also found that the normalized values of M_s at room temperature are function of the Fe metallic particle size. Finally, we have found that the magnetic anisotropy constant of superparamagnetic Fe nanoparticles depend on the nature of their coating shell.

DOI: 10.1103/PhysRevB.69.094401 PACS number(s): 75.75.+a

I. INTRODUCTION

Nanocrystalline magnetic materials often reveal unique properties that differ from their bulk polycrystalline counterparts. Interest in this area comes partly from data storage technology (e.g., hard disk drives[1]), partly from biotechnology,[2] and partly because nanomagnets provide a highly controlled experimental system for studying fundamental phenomena in physics.[3]

A particularly interesting physics occurs when nanomagnets are dispersed in a matrix.[4] The magnetic behavior of these systems can vary widely depending on the size of the nanocrystalline particles as well as on the packing fraction and the interaction between the nanomagnets and the matrixes.[5–7] For an assembly of noninteracting fine particles the magnetic behavior is understood on the basis of Néel arguments that led to the concept of superparamagnetism, namely, the reversal of their magnetization through a thermally activated process over the anisotropy barrier, even in the absence of an externally applied field. For sufficiently dilute dispersions, interparticle interactions are negligible and the crossover to the blocked state with decreasing temperature depends only on the physical properties of the individual particles. When the interparticle interactions become significant the behavior of a magnetic moment is not only governed by its own intrinsic anisotropy energy but also by the coupling with its neighbors. Although it has been studied very intensively, it remains unclear how the magnetic interactions affect the magnetic behavior of nanoscopic systems. Dipolar interactions cause a frustration of the moments. In addition, there is a frustration resulting from the competition between the interparticle dipolar and exchange terms and the intraparticle anisotropy energy that requires the magnetization vector to be aligned along specific axes in each particle.[8] When the interactions are strong enough, the particles may behave as a spin glass,[9] although a true phase transition needs the combined effects of dipolar interaction and anisotropy.[10]

A knowledge of these fundamental properties is essential for the creative use of nanomagnetic composites than can have tremendous potential and lead to improved materials for applications in biology and medicine for the separation of biochemical products and cells,[11] magnetic resonance imaging contrast enhancement,[12] and a tissue specific release of therapeutic agents.[13] All of these applications depend on a magnetic material with a modified surface that provides functionality to the composite. In this way, the dispersion of nanomagnets in silica matrixes that can be easily activated[14] to provide functionality to the magnetic material seems the ideal encapsulating material. In addition, the silica matrix greatly enhances the wear and corrosion resistance of the magnetic nanoparticles, and allows a fine tuning with temperature of the magnetic properties.[15]

Herein we report a study of the magnetic behavior of superparamagnetic Fe metallic nanocrystals (4–7 nm) confined inside submicron-sized spherical silica cages (average size ~150 nm in diameter) that could find applications in the magnetically assisted chemical separation of biochemical products. Because this application requires the preparation of stable liquid suspensions of magnetic particles, the ideal microstructure must consist of magnetic nanocrystals dispersed in submicron-sized diamagnetic spherical particles that are expected to have long sedimentation times in the absence of a magnetic field. The composites were prepared by an aerosol-assisted method that was recently reported to be adequate for the preparation of γ-Fe_2O_3 nanocrystals confined within diamagnetic matrixes.[16] Considering the complexity of the system, before magnetic characterization, a crucial as-

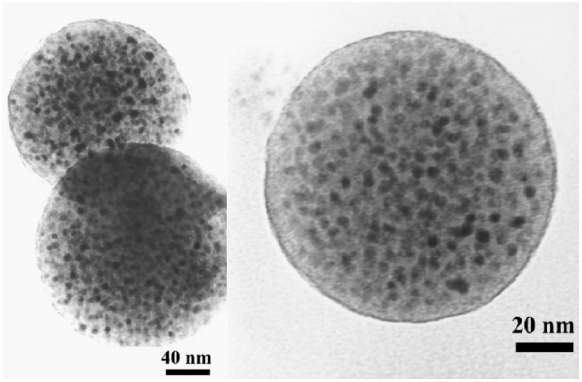

FIG. 1. Typical TEM microstructures of Fe nanocrystals confined inside submicron sized spherical silica particles. The dark spots correspond to the nanoparticles containing the α-Fe metallic core.

pect we have addressed is the detailed crystallochemical characterization of samples. For example, it is known that some production methods guarantee nonmagnetic oxide layers around each magnetic core (cluster, particle, or granule) while others allow the cores to come into direct contact. This can make a profound difference in the magnetic properties since the shell can exclude the direct exchange interaction between particles so that the dipole force dominates at all achievable volume fractions. If, on the other hand, the magnetic metallic clusters are allowed to touch, exchange interactions could take place even at low volume fractions.[3] Further complication arises from the use of methods, such as ball milling, that favor the presence of structurally disordered grain boundaries showing a spin-glass-like behavior.[17] Since the boundary spins are frozen in random directions the exchange interaction cannot be transmitted across the interfaces.

II. EXPERIMENTAL PROCEDURE

Fe nanocrystals confined inside submicron spherical silica particles were obtained by an aerosol-assisted method. First, we prepared γ-Fe_2O_3 nanocrystals confined in spherical silica cages. Details of the preparation of the γ-Fe_2O_3/silica composites can be found elsewhere.[15,16] Here it is sufficient to say that the powders generated after the aerosol pyrolysis of a solution containing $Fe(NO_3)_3 \cdot 9H_2O$, tetraethoxysilane and methanol were heated at different temperatures (800–1000 °C) in air to obtain composites containing γ-Fe_2O_3 nanocrystals of different sizes. Fe nanocrystals confined inside submicron spherical silica particles were obtained after reducing the γ-Fe_2O_3/silica composites to α-Fe in a H_2 atmosphere at 500 °C for 10 h and cooled to room temperature under the hydrogen atmosphere.

Phase identification was carried out by x-ray diffraction (XRD) in a Philips PW1710 using Cu$K\alpha$ radiation. Fe crystallite sizes were estimated from the full width at half maximum of the reflection (110) of α-Fe by using the Scherrer equation. Particle size and shape of the samples were examined by transmission electron microscopy (TEM, Jeol 2000 FX). ^{57}Fe Mössbauer absorption spectroscopy was used to characterize the samples. The spectra were recorded with a maximum velocity of 10 mm s^{-1} at different temperatures with a ^{57}Co:Rh source. Magnetic properties of the samples were recorded in a vibrating sample magnetometer (MLVSM9 MagLab 9 T, Oxford Instrument). The saturation magnetization (M_s) and coercivity field values (H_c) were obtained from the hysteresis loops registered up to a field of 5T. M_s values were obtained from the law of approach to saturation.[18]

TABLE I. Total amount of Fe present in samples and phase composition in wt % as determined by Mössbauer spectroscopy. Uncertainties in the weight composition were about 5%.

Sample	F1	F2	F3	F4
$Fe/(Fe+SiO_2)$ (wt %)	15	15	15	25
α-Fe	6	4	3	12
Fe_2SiO_4	8	11	13	13
Fe_2O_3	5	5	5	7
SiO_2	81	80	79	68

III. RESULTS AND DISCUSSION

A. Crystallochemical characteristics of samples

After reduction (see Sec. II for details) the samples consisted of iron nanocrystals (XRD only showed diffraction peaks due to α-Fe) distributed inside the submicron sized spherical silica particles (Fig. 1). In order to study size and interparticle effects, composites with different Fe particle sizes and Fe/silica compositions were prepared. A summary of the main physical characteristics of samples can be found in Tables I and II. It is worthy of note that composites with a lower load of magnetic material were not prepared because, as we will see below, the content in α-Fe was very low. On

TABLE II. α-Fe crystallite size (D_{XR}) and values of M_S at RT normalized to the α-Fe content in samples. Values of the median blocking temperature $\langle T_B \rangle$ and the standard deviation σ_y obtained from the fit of the decay of the reduced remanence. The uncertainties are about 1–2 K for $\langle T_B \rangle$ and 0.1 for σ_y. The values of the mean blocking temperature T_m and the anisotropy constant K_R derived from T_m are also shown. The uncertainties in T_m and K_R were obtained from the uncertainties in $\langle T_B \rangle$, σ_y, and the particle diameter. Finally, the values of the magnetic anisotropy constant K_{LAS} determined from the law of approach to saturation and the values of H_c at 5 K are also shown.

Sample	F1	F2	F3	F4
D_{XR} (nm)	6.9 (0.5)	5.2 (0.5)	4.4 (0.5)	7.3 (0.5)
M_S (emu/g Fe)	205	180	160	210
$\langle T_B \rangle$ (K)	61	29	19	66
σ_y	0.95	0.95	1.00	1.00
T_m (K)	25 (5)	13 (3)	7 (2)	24 (6)
K_R ($\times 10^4$ J m^{-3})	5 (2)	6 (3)	5 (4)	4 (2)
K_{LAS} ($\times 10^4$ J m^{-3})	5.4	6.9	7.7	5.3
H_c (Oe)	450	390	330	490

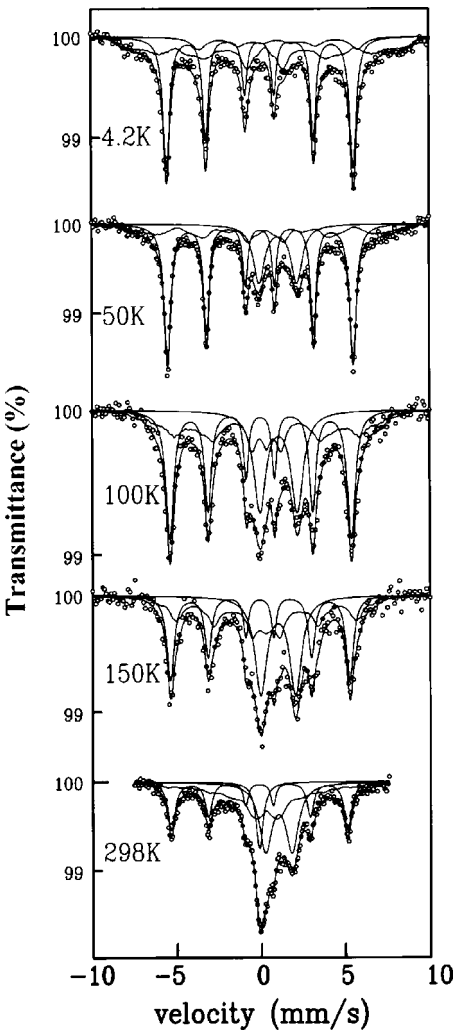

FIG. 2. Mössbauer spectra for sample F1.

the other hand, a higher load of magnetic material led to composites in which some uncontrolled interparticle sintering was observed.

XRD cannot discard the presence of other phases such as the iron oxide spinel normally formed during α-Fe corrosion processes.[19,20] This phase normally appears in the form of nanocrystals of about 2 nm in size (with a grain size lower than $\sim$2 nm, diffraction effects are diffuse and close to the background noise) that combined with their low content could be the reason for their absence in the XRD patterns. Alternatively, because the reduction is carried out inside a silica matrix, we cannot disregard the presence of an outer shell of iron (II) silicate surrounding the inner Fe metallic core. Therefore, we registered the Mössbauer spectra of the samples to determine the possible presence of any other iron-containing phase apart of α-Fe.

Figure 2 shows the Mössbauer spectra of sample F1 (chosen as representative) registered at different temperatures. The other samples showed similar spectra only with differences in the relative amount of phases. It is worthy of note that we have assumed similar effective Debye-Waller factors for all the different phases present on the samples as previously assumed by Hadjipanayis and co-workers when working on a similar system.[21,22] Recently Kuhn *et al.* confirmed the validity of this assumption also for a similar system.[19] At room temperature (RT) the spectrum consists of a single line with an isomer shift of 0.0 mm s^{-1} that is due to the presence of a fraction of superparamagnetic α-Fe particles, and a sextet with an isomer shift of 0.0 mm s^{-1}, a quadrupole splitting of 0.0 mm s^{-1}, and a hyperfine field of 32.5 T, which corresponds to the fraction of α-Fe particles that are blocked at RT. The fraction of α-Fe particles that remains superparamagnetic is about 30% for this sample. Supporting the presence of superparamagnetic α-Fe at RT, samples F2 and F3, that according to XRD contain Fe nanocrystals with a mean size smaller than sample F1 (5.2 nm for sample F2 and 4.4 nm for sample F3 versus 6.9 nm for sample F1), have a larger fraction of superparamagnetic α-Fe particles at RT (60% for sample F2 and 70% for sample F3). Moreover, the fraction of α-Fe particles that remains superparamagnetic in sample F4 that have a similar crystallite size was similar (30%).

The Mössbauer spectrum at RT also displays the presence of a doublet with an isomer shift of 1.04 mm s^{-1} and a quadrupole splitting of 1.59 mm s^{-1} that is characteristic of high-spin Fe (II) cations in octahedral coordination. It arises most likely from the nanoparticle/silica interface, where Fe (II) cations exist in an environment similar to that of Fe_2SiO_4.[22,23] In accordance with this interpretation, the relative content of this phase increase with the decrease of the iron core crystallite size (smaller particle sizes involve larger surface areas and therefore larger contact area). Finally, the spectrum displays a non-resolved sextet (mainly consisting of a central broad quadrupolar doublet) with an isomer shift of 0.4 mm s^{-1} that could be associated with the presence of ferric oxide nanoparticles. The fact that the relative content of this phase was independent of particle size, i.e., surface area (see, in Tables I and II, samples F1, F2, and F3) seems to suggest that its presence is due to the incomplete reduction of the samples rather to the presence of an iron oxide corrosion layer formed during passivation processes.

In order to further elucidate the nature of the phases present on the samples, we registered the spectra of sample F1 at lower temperatures (Fig. 2). At 150 K, the spectrum displays a sextet associated with α-Fe. However, no single line associated with superparamagnetic Fe nanocrystals is detected, which means that all Fe nanocrystals are blocked (according to Mössbauer) at this temperature. The spectrum also displays a sextet with an isomer shift of 0.37 mm s^{-1} that can only be fitted to a distribution of hyperfine fields. This signal corresponds to the ferric oxide nanoparticles. Finally, the spectrum displays the doublet associated with Fe (II) cations in an environment similar to that of Fe_2SiO_4. At 100 K, the spectrum is similar to that observed at 150 K; the only difference is that the sextet associated with ferric oxide nanoparticles appears better resolved.

At 50 K, the most significant result is that we observe a decrease in the doublet associated with Fe_2SiO_4 from 30 to 20%. This decrease is more evident at 4.2 K, where the signal associated with Fe_2SiO_4 represents only a 10%, while the one associated with α-Fe increases from 36% to 50% and the one associated with ferric oxide increases from 32% to 40%.

Fe_2SiO_4 is antiferromagnetic and has an associated Néel temperature of 65 K.[24] Thus, at temperatures below 65 K we should observe the signal associated with the magnetic hyperfine splitting. Moreover, because of the small particle size, we must have a significant fraction of this phase that remains superparamagnetic especially at 50 K. However, the magnetic hyperfine fields of Fe (II) components are very sensitive to local distortions caused by, for example, defects, because of the orbital contribution to the magnetic hyperfine field. Therefore, if there are variations of the local environment of the Fe (II) cations, the Fe (II) components may be smeared out such they are not visible as separate components,[19] and this could be the reason we can only observe the fraction of the Fe_2SiO_4 that remains superparamagnetic. Finally, it is worthy of note that the value of the hyperfine field obtained for the α-Fe metallic core at 4.2 K (34.0 T) is similar to that obtained for pure α-Fe (33.9 T),[25] which excludes the possibility of having silicon atoms forming a Fe-Si alloy. A summary of the phase composition of samples obtained from the Mössbauer analyses can be found in Table I.

The temperature variation of the spectral features described above and the hyperfine parameters of the spectral components derived from the fit suggest two possible scenarios to represent the iron-containing nanoparticles encapsulated in the spherical silica particles: (1) The nanoparticles consist of an inner central core of the iron oxide that remains unreduced, surrounded by an outer central core of α-Fe that is encapsulated in an outer shell of Fe_2SiO_4; (2) we have nanoparticles consisting of an α-Fe core that is encapsulated in a Fe_2SiO_4 shell, and separately we have iron oxide nanoparticles that remain unreduced. These iron oxide nanoparticles are most likely located close to the center of the bigger spherical silica particles and thus are difficult to reduce. It is worth mentioning that more severe thermal treatments to fully accomplish the reduction of the composites have not been studied because they drive to uncontrolled interparticle sintering. Independently of which of the two scenarios better represents the distribution of the iron-containing phases, it is clear that in our system we can exclude α-Fe metallic cores from coming into contact, and thus direct exchange interactions can be discarded. In this way, their magnetic response must be the result of a competition between intraparticle anisotropy and interparticle dipolar interactions.

B. Magnetic behavior of samples

In data storage applications, the particles must have a stable, switchable magnetic state to represent bits of information, a state that cannot be affected by temperature fluctuations, for example. However, for biomedical applications the use of particles that present a superparamagnetic behavior at room temperature (no remanence along with a rapidly changing magnetic state) is preferred.[26] In order to check for superparamagnetic behavior, we registered the hysteresis loop at RT in our samples (Fig. 3). We can clearly see that the particles are superparamagnetic (i.e., the value of H_c is zero).[27] Samples containing Fe nanocrystals of sizes larger than those here presented ($\geqslant 8$ nm) did not show a superparamagnetic behavior at RT and thus were not studied.

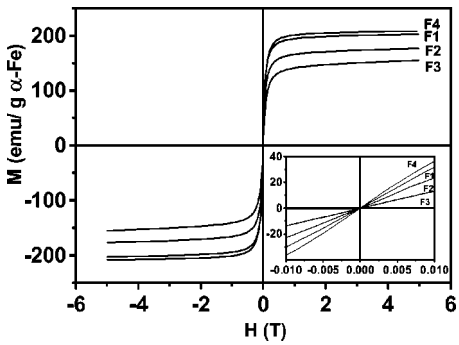

FIG. 3. Hysteresis loops of samples at RT. The inside plot is a magnification of M-H at low magnetic field (from -0.01 to 0.01 T) to show the superparamagnetic behavior of the composites (zero coercivity field). Values of M were normalized to the α-Fe content.

For iron nanocrystals between 4 and 7 nm we expect the M_s values to be similar to those of bulk (220 emu/g) at temperatures of about 5 K,[17,28] and indeed this was the case when the α-Fe content, obtained by quantitative analyses of the Mössbauer spectra at RT and 150 K to assure that all the Fe_2SiO_4 is visible, was used to determine the normalized M_s values for all the samples. In addition, this result seems to suggest that the estimation of the phase content on samples by Mössbauer was reliable. On the other hand, these M_s values at RT (Table II) were, in all cases, lower than that of bulk Fe, which reflects the small particle size of the Fe nanocrystals. Theoretical calculations on ferromagnetic clusters carried out by Hendriksen *et al.*[29] have shown that a finite particle size can cause a sizable deviation from the normal Bloch $T^{3/2}$ law and that the Curie temperature can be reduced for the smallest particles.[30] Supporting this interpretation the normalized M_s values at RT increased as the crystallite size increased (in fact for the samples with a crystallite size about 7 nm were closed to the bulk value) and for the samples with different composition but similar crystallite size were similar (Table II). It is worthy of note that the values of M_s remained almost invariant after six months, i.e., the samples were stable, which is probably due to the combined effect of the silica matrix and the iron (II) silicate protective layer.

As mentioned above, a possible use of these particles is in the biomedicine field. Therefore, it could be of interest to check for the presence of dipolar interactions between the superparamagnetic nanomagnets confined inside the spherical silica particles to better predict the magnetic response of these composites. A comprehensive analysis of the possible presence of dipolar interactions was carried out with the help of a mean-field model, recently proposed by Allia *et al.*[31] and later on verified by Binn *et al.*[3] The use of this model could allow us to estimate dipolar interactions at a temperature region, in which the so-called interacting superparamagnetic regime describes the behavior of interacting nanomagnets. In particular, in this region dipolar interactions can be characterized by a parameter T^*, appearing in the denominator of a modified Langevin function analogous to the Curie-Weiss law:

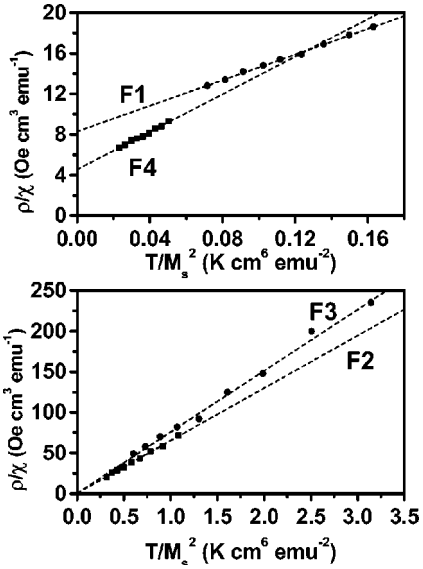

FIG. 4. Variation of the quantity ρ/χ on the ratio T/M_S^2 for all samples in a temperature range from 200 to 400 K. The solid line represents the best linear fit of the data using Eq. (3).

$$M = N\mu L\left(\frac{\mu H}{k(T+T^*)}\right), \tag{1}$$

where N is the number of moments per unit volume, μ is the particle moment, L is the Langevin function, k is the Boltzmann constant, H is the applied magnetic field, and T is the temperature. The parameter T^* is proportional to the dipolar energy and can be obtained from the following expression:[31]

$$T^* = \frac{\alpha}{k}\frac{M_S^2}{N}, \tag{2}$$

where α is a proportionality constant deriving from the sum of all dipolar energy contributions,[32] N is the number of moments per unit volume and k is the Boltzmann constant. α and N can obtained from the low-field susceptibility data, χ, using the expression

$$\frac{\rho}{\chi} = 3kN\left(\frac{T}{M_S^2}\right) + 3\alpha. \tag{3}$$

We have assumed a log-normal distribution to estimate ρ in Eq. (3). The use of this type of distribution to describe systems containing magnetic nanocrystals has been previously shown to be adequate.[33] If our system follows the ISP regime in a particular range of temperatures, we can expect a linear dependence of the quantity ρ/χ on the ratio T/M_S^2 and we can easily obtain the values of α and N (hence T^*). The linear dependence of the quantity ρ/χ on the ratio T/M_S^2 is clearly displayed in Fig. 4 for all samples.[34] This result supports a picture of an interacting superparamagnetic regime as recently reported in similar nanostructured systems. This ISP regime appears as an intermediate regime, separating the high-temperature, conventional superparamagnetic regime from the low temperature, blocked-particle regime. The values of T^* at 300 K obtained from the best linear fits were lower for sample F1 (360 K) than for sample F4 (450 K), which correlates well with the lower Fe content of sample F1. In the composites having the smaller Fe nanoparticle sizes and the lower volume fractions (F2 and F3), the dipolar interactions were weaker, and thus at RT the values of T^* for these two samples were close to zero, i.e., the composites behave as an ideal superparamagnet. However, at lower temperatures we can expect a transition from an ideal superparamagnetic regime to an interacting superparamagnetic regime, as reported in similar nanostructured systems.[3,31] Further confirmation of the occurrence of interparticle interactions in the composites were obtained after analyzing the low temperature variation of the coercivity. In the absence of interactions, the coercivity should follow the well-known expression $H_C(T) = H_C(0)[1-(T/T_B)^{1/2}]$.[35] In our samples we do not observe this dependence (Fig. 5), which is in accordance with the occurrence of interparticle interactions in all the characterized composites.[36]

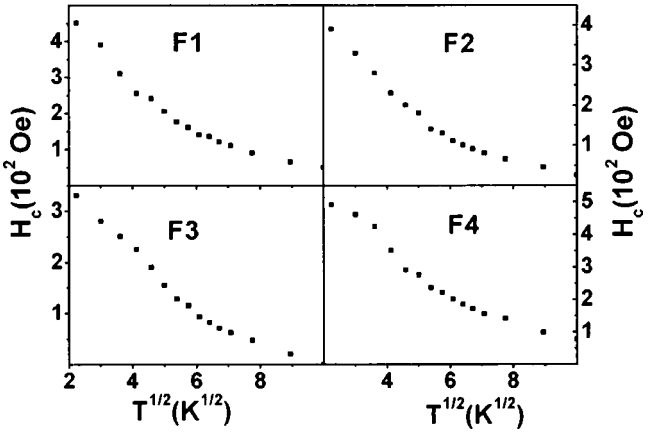

FIG. 5. Variation of H_c with $T^{1/2}$ for all the samples. The nonlinear behavior clearly discards the $\frac{1}{2}$ thermal dependence of the coercivity.

El-Hilo *et al.*[37] found that the blocking temperatures, obtained from measurements of isothermal remanence for ferrofluids with different concentrations of 8-nm iron oxide particles, were nearly identical, and they concluded that the decay of remanence was not sensitive to interaction effects. Moreover, Mørup *et al.*,[9] also working with γ-Fe_2O_3 nanocrystals of about 8 nm coated and uncoated with a layer of oleic acid, showed similar results. Only for the case of an uncoated powder pressed at about 1300 MPa did these authors note a slight increase in the blocking temperature that they associated with interaction effects. In our samples, according to Mössbauer, the iron nanocrystals are coated by an iron (II) silicate shell. Moreover, the α-Fe volume packing fraction is very low, and therefore we could expect that the blocking temperatures estimated from the variation of the reduced remanence must be insensitive to interaction effects. Figure 6 shows the reduced remanence data as a function of temperature for all the samples. We have analyzed the results using the standard relation for the temperature variation of the reduced remanence (normalized to the measured saturation magnetization), which allows one, among other things,

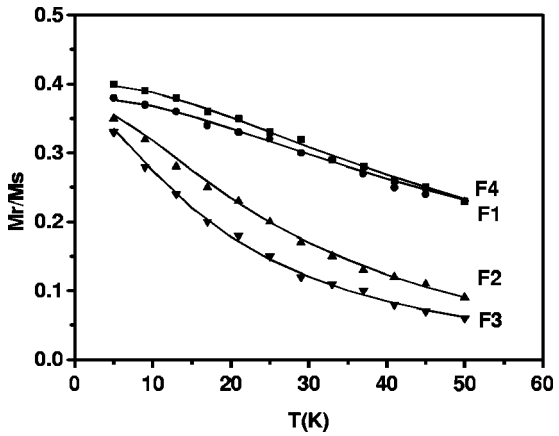

FIG. 6. Variation of the reduced isothermal remanence with temperature for all the samples. The solid lines represent the best fit of the data with a standard decay-of-remanence model.

to obtain quantitative information about the mean blocking temperature. The relation is given by

$$\frac{M_R(T)}{M_S(T)} = \frac{M_R(0)}{M_S(0)} \int_{T/\langle T_B \rangle}^{\infty} f(y)dy, \tag{4}$$

where $\langle T_B \rangle$ is the median blocking temperature, $y = T_B/\langle T_B \rangle$ is the reduced blocking temperature, and $M_R(0)/M_S(0)$ is the reduced remanence at 0 K. The distribution $f(y)$ of reduced blocking temperatures is assumed to be a log-normal function:

$$f(y) = \frac{1}{(2\pi)^{1/2} y \sigma_y} \exp\left[-\frac{(\ln y)^2}{2\sigma_y^2} \right]. \tag{5}$$

The best fits with Eq. (4) to the data are shown by the lines in Fig. 6, and the values of $\langle T_B \rangle$ and the standard deviation σ_y are given in Table II. From the values of $\langle T_B \rangle$ and the standard deviation σ_y, we can obtain the mean value of the blocking temperature using the expression $T_m = \langle T_B \rangle \exp(-\sigma_y^2)$. As expected, the values of T_m (Table II) increased with the increase of particle size, and, for samples with similar particle sizes but different volume packing fractions, the values of T_m remained unchanged (as predicted the decay of remanence is mainly determined by anisotropy). From the values of T_m and particle size obtained by XRD, we can make an estimation of the magnetic anisotropy constant K using the expression $KV = k_B T_B \ln(\tau_m/\tau_0)$, where V is the particle volume, k_B is the Boltzmann constant, τ_0 is the characteristic time, and τ_m is the measuring time. Considering the typical values for τ_0 and assuming $\tau_m \sim 100$ s for a measurement carried out in a vibrating sample magnetometer,[28,37] the values of the magnetic anisotropy constant (Table II) are very similar for all samples and close to the value reported for bulk Fe (4.8×10^4 J m^{-3}).[18] However, the experimental uncertainties preclude us to discard small variations in the values of the anisotropy constant. Thus, attempts were made to determine more precisely the anisotropy constant. Particularly, we determined the value of K from the magnetization data at 5 K using the law of approach to saturation:[18]

$$M = M_S\left(1 - \frac{B}{H} - \frac{C}{H^2}\right) + \chi_f H, \tag{6}$$

where M_S is the saturation magnetization, χ_f is the high-field susceptibility, and B is function of M_S and K, and is given by the following expression:[38]

$$B = \frac{4 S_B K_{\text{eff}}^2}{15 M_S^2}. \tag{7}$$

The obtained values (Table II) are close to the bulk value for samples F1 and F4 while an increase is observed in samples F2 and F3.[39] In any case, the enhancements of the anisotropy value observed in our samples with respect to the bulk were smaller to that reported in iron nanoparticles that consisted of a α-Fe metallic core and an iron oxide passivation shell[21] (5×10^5 J m^{-3}, ~ 1 order of magnitude). This increase was associated with the interaction between the iron oxide passivation shell and the Fe metallic core. In our system, as determined by Mössbauer spectroscopy, apart from the presence of ferric oxide, we have the metallic Fe surrounded by an appreciable amount of an iron (II) silicate protective layer. Therefore, we could expect the interaction between the metallic core and the surface of these two systems to be different. Particularly, it seems that in our system this interaction is weaker. Alternatively, we can speculate that the observed enhancement in the anisotropy constant of the Fe nanoparticles coated by an iron oxide passivation layer (normally γ-Fe_2O_3 or Fe_3O_4) (Ref. 19) could have some contribution from the iron oxide itself. In fact, enhancements of two orders of magnitude (from 4.8×10^3 J m^{-3} of bulk maghemite to $\sim 5 \times 10^5$ J m^{-3}) have been observed in γ-Fe_2O_3 nanoparticles, and have been associated with the existence of a magnetically disordered surface layer.[40,41]

A further confirmation of the veracity of the anisotropy constant values was obtained from the values of H_c at 5 K (Table II). For example, for an assembly of noninteracting randomly oriented single-domain cubic particles the value of coercivity can be determined by the expression $H_C = 0.64K/M_s$ (200–300 Oe for the range of anisotropy constants determined by the law of approach to saturation), while for uniaxial particles $H_C = 0.96K/M_s$ (300–450 Oe for the range of anisotropy constants determined by the law of approach to saturation). Variations with respect to these theoretical values can be associated for example with interparticle interactions or interactions between the Fe nanoparticles and the matrix.[42] Finally, it is worth mentioning the decrease in H_c values with decreasing particle size, which could reflect the presence in composites having smaller Fe nanoparticles of a fraction of composites that remains unblocked at 5 K. In fact, as observed in the variation of the reduced isothermal remanence with temperature (Fig. 6) the values at 5 K for samples F2 and F3 were smaller. Alternatively, we cannot discard some slight contribution from anisotropy shape in the samples having bigger sizes.

IV. SUMMARY AND CONCLUSIONS

Mössbauer studies have allowed us to determine that the magnetic response of iron nanoparticles dispersed in submicron-sized silica particles must be the result of a competition between intraparticle anisotropy and interparticle dipolar interactions. We have also found that in our system a superparamagnetic behavior at RT is found for Fe nanocrystals below about 8 nm in diameter. However, studies of the thermal dependence of the magnetization have shown evidence of an interacting superparamagnetic regime in our samples, as recently observed in similar nanostructured systems. We have also found a dependence of the values of M_s with the Fe particle size at RT. Finally, we have determined that the enhancements of the anisotropy values observed in our samples with respect to the bulk were smaller that reported in iron nanoparticles that only consisted of a Fe metallic core and an iron oxide passivation shell. The reason, therefore, for this discrepancy could be either associated with the presence in our samples of an iron (II) silicate shell coating the Fe metallic core or to the lower relative content of a ferrimagnetic iron oxide layer.

ACKNOWLEDGMENTS

Financial support from CICYT (MAT2002-04001-C02) is gratefully acknowledged. P. T. thanks the financial support from the Ramon y Cajal program.

*Author to whom correspondence should be addressed. FAX: 34-91-3720623. Electronic address: ptartaj@icmm.csic.es

[1] S. H. Sun, C. B. Murray, D. Weller, L. Folks, and A. Moser, Science **287**, 1989 (2000).
[2] M. Zhao, L. Josephson, Y. Tang, and R. Weissleder, Angew. Chem., Int. Ed. **42**, 1375 (2003).
[3] X. Batlle and A. Labarta, J. Phys. D: Appl. Phys. **35**, R15 (2002).
[4] C. Binns, M. J. Maher, Q. A. Pankhurst, D. Kechrakos, and K. N. Trohidou, Phys. Rev. B **66**, 184413 (2002).
[5] S. H. Liou and C. L. Chien, Appl. Phys. Lett. **52**, 512 (1988).
[6] D. Kumar, J. Narayan, A. V. Kvit, A. K. Sharma, and J. Sankar, J. Magn. Magn. Mater. **232**, 161 (2001).
[7] P. Katiyar, D. Kumar, T. K. Nath, A. V. Kvit, J. Narayan, S. Shattopadhyay, W. M. Gilmore, S. Coleman, C. B. Lee, J. Sankar, and R. K. Singh, Appl. Phys. Lett. **79**, 1327 (2001).
[8] G. A. Held, G. Grinstein, H. Doyle, S. Sun, and C. B. Murray, Phys. Rev. B **64**, 012408 (2002).
[9] S. Mørup, F. Bødker, P. V. Hendriksen, and S. Linderoth, Phys. Rev. B **52**, 287 (1995).
[10] J. García-Otero, M. Porto, J. Rivas, and A. Bunde, Phys. Rev. Lett. **84**, 167 (2000).
[11] J. T. Kemshead, J. G. Treleaven, F. M. Gibson, J. Ugllstad, A. Rembaum, and T. Philip, Prog. Exp. Tumor Res. **29**, 249 (1985).
[12] C. W. Jung and P. Jacobs, Magn. Reson. Imaging **13**, 661 (1995).
[13] P. K. Gupta and C. T. Hung, Life Sci. **44**, 175 (1989).
[14] A. Ulman, Chem. Rev. **96**, 1533 (1996).
[15] P. Tartaj, T. González-Carreño, and C. J. Serna, Adv. Mater. **13**, 1620 (2001).
[16] P. Tartaj, T. González-Carreño, and C. J. Serna, Langmuir **18**, 4556 (2002).
[17] E. Bonetti, L. Del Bianco, D. Fiorani, D. Rinaldi, R. Caciuffo, and A. Hernando, Phys. Rev. Lett. **83**, 2829 (1999).
[18] B. D. Cullity, *Introduction to Magnetic Materials* (Addison-Wesley, Reading, MA, 1972).
[19] L. Theil Kuhn, A. Bojsen, L. Timmerman, M. Meedom-Nielsen, and S. Mørup, J. Phys.: Condens. Matter **14**, 13551 (2002).
[20] L. Del Bianco, D. Fiorani, A. M. Testa, E. Bonetti, L. Savini, and S. Signoretti, Phys. Rev. B **66**, 174418 (2002).
[21] S. Gangopadhyay, G. C. Hadjipanayis, B. Dale, C. M. Sorensen, K. J. Klabunde, V. Papaefthymiou, and A. Kostikas, Phys. Rev. B **45**, 9778 (1992).
[22] V. Papapefthymiou, A. Tsoukatos, G. C. Hadjipanayis, A. Simopoulos, and A. Kostikas, J. Magn. Magn. Mater. **140-44**, 397 (1995).
[23] D. P. Yang, Y. D. Zhang, and S. Hui, J. Appl. Phys. **91**, 8198 (2002).
[24] S. S. Hafner, J. Stanek, and M. Stanek, J. Phys. Chem. Solids **51**, 203 (1988).
[25] O. F. Bakkaloglu, M. F. Thomas, R. J. Pollar, and P. J. Grundy, J. Magn. Magn. Mater. **125**, 221 (1993).
[26] P. Tartaj, M. P. Morales, S. Veintemillas-Verdaguer, T. Gonzalez-Carreño, and C. J. Serna, J. Phys. D: Appl. Phys. **36**, R182 (2003).
[27] This result is not surprising because we had already observed by Mössbauer that a significant fraction of the α-Fe nanoparticles was superparamagnetic at RT (Fig. 2). When using Mössbauer spectroscopy, the superparamagnetic relaxation results in a broadening of the absorption lines for relaxation times of the order of 10^{-8} s, and the magnetic hyperfine splitting disappears for relaxation times $\leqslant 10^{-9}$ (see, for example, Ref. 9). Meanwhile measuring times in a VSM are about 100 s (see, for example, Ref. 35). Thus, we could expect superparamagnetic behavior in all our samples when registering the hysteresis loops.
[28] F. Bødker, S. Mørup, and S. Linderoth, Phys. Rev. Lett. **72**, 282 (1994).
[29] P. V. Hendriksen, S. Linderoth, and P. A. Lingard, Phys. Rev. B **48**, 7259 (1993).
[30] A. T. Ngo, P. Bonville, and M. P. Pileni, J. Appl. Phys. **89**, 3370 (2001).
[31] P. Allia, M. Coisson, P. Tiberto, F. Viani, M. Knobel, M. A. Novak, and W. C. Nunes, Phys. Rev. B **64**, 144420 (2001).
[32] C. Kittel, *Introduction to Solid State Physics* (Wiley, New York, 1968).
[33] K. O'Grady and A. J. Bradbury, J. Magn. Magn. Mater. **39**, 91 (1983).
[34] In doing this fit we have assumed that the contribution of the ferrimagnetic iron oxide to the total magnetization can be discarded. This assumption is based on previous studies on ferrimagnetic iron oxide nanoparticles of about 2 nm or lower (as above mentioned, the fact that this phase was not detected by XRD suggest a crystallite size of about these values) that showed values of saturation magnetization of pure ferrimagnetic iron oxide nanoparticles about 5 emu/g (see, for example, Refs. 15 and 40). Spin canting has been associated with this strong reduction of magnetization with respect to the bulk phase in

ferrimagnetic iron oxides. Also, on doing the fit the volume fraction of α-Fe was estimated from the Mössbauer data.

[35] Recently, Fonseca *et al.* observed the $\frac{1}{2}$ thermal dependence of coercivity in non-interacting Ni nanoparticles embedded in a massive silica matrix [F. C. Fonseca, G. F. Goya, R. F. Jardim, R. Mucillo, N. L. V. Carreño, E. Longo, and E. R. Leite, Phys. Rev. B **65**, 104406 (2002)].

[36] It is worthy of note that for an assembly of aligned particles, a 0.77 thermal dependence of the coercivity instead a 0.5 is predicted. However, TEM micrographs displayed in Fig. 1 indicate that the Fe nanocrystals are randomly distributed in the submicron-sized silica matrix. In any case, we also tried to fit the thermal dependence of the coercivity using 0.77 instead 0.5 and did not obtain better fits.

[37] M. El-Hilo, K. O'Grady, and R. W. Chantrell, J. Magn. Magn. Mater. **114**, 295 (1992).

[38] H. Kojima, in *Ferromagnetic Materials*, edited by E. P. Wohlfarth (North-Holland, Amsterdom, 1982), Vol. 3.

[39] The measurements were sensitive to the field interval of the $M(H)$ curves fitted using the law of approach to saturation, since it is very difficult to separate the contribution of B/H and C/H^2, and a variation of 10–20 % was found.

[40] B. Martinez, A. Roig, E. Molins, T. González-Carreño, and C. J. Serna, J. Appl. Phys. **83**, 3256 (1998).

[41] O. Iglesias and A. Labarta, Phys. Rev. B **63**, 184416 (2001).

[42] M. Alonso-Sañudo, J. J. Blacwell, K. O'Grady, J. M. González, F. Cebollada, and M. P. Morales, J. Magn. Magn. Mater. **221**, 214 (2000).